Boosting intermolecular interactions of fused cyclic explosives: the way to thermostable and insensitive energetic materials with high density

Xiang Chen,[a] Zhaoqi Guo,[a] Cong Zhang,[a] Jianguo Zhang,[b] and Haixia Ma*[a]

[a.] School of Chemical Engineering / Xi'an Key Laboratory of Special Energy Materials, Northwest University, Xi'an 710069, Shaanxi, P. R. China. E-mail: mahx@nwu.edu.cn.

[b.] State Key Laboratory of Explosion Science and Technology, Beijing Institute of Technology, Beijing 100081, P. R. China.

Table of Contents

1. Crystallographic data and crystal structures

Table S1. Crystallographic data for **1**, **1b·H_2O**, **2**, **2e·H_2O**

Compound	**1**	**2**	**1b·H_2O**	**2e·H_2O**
Empirical formula	$C_3H_2N_6O$	$C_3H_3N_7O$	$C_3H_7N_7O_2$	$C_4H_{10}N_{10}O_2$
Temperature/K	296(2)	141(2)	296(2)	296(2)
Crystal system	monoclinic	monoclinic	monoclinic	triclinic
Space group	*Cc*	$P2_1/n$	*Cc*	*P*1
a/Å	12.6514(15)	8.621(3)	4.0295(11)	3.7934(4)
b/Å	5.2884(6)	14.613(5)	12.201(3)	7.4317(7)
c/Å	7.4471(8)	8.627(3)	14.678(4)	8.7328(8)
α/°	90	90	90	105.198(5)
β/°	92.903(4)	97.998(12)	91.823(10)	100.874(5)
γ/°	90	90	90	92.381(5)
V/Å^3	497.61(10)	1076.2(6)	721.2(3)	232.24(4)
Z	4	8	4	1
ρ/g·cm^{-3}	1.843	1.890	1.595	1.646
μ/mm^{-1}	0.149	0.153	0.134	0.135
F(000)	280.0	624.0	360.0	120.0
2θ range/°	12.384 to 53.996	5.524 to 52.928	7.234 to 69.7	4.94 to 55.108
Reflns. collected	1552	2197	4877	3223
Indep. reflns.	827	2197	2185	1933
Data/restraints/parameters	827/2/92	2197/0/216	2185/5/127	1933/6/151
GOOF	1.066	1.099	1.083	1.153
Final R^a indexes [I>=2σ(*I*)]	R_1 = 0.0244, wR_2 = 0.0639	R_1 = 0.0385, wR_2 = 0.0847	R_1 = 0.0622, wR_2 = 0.1545	R_1 = 0.0468, wR_2 = 0.0993
Final *R* indexes [all data]	R_1 = 0.0247, wR_2 = 0.0641	R_1 = 0.0601, wR_2 = 0.0994	R_1 = 0.0680, wR_2 = 0.1592	R_1 = 0.0575, wR_2 = 0.1044
Recrystallization solvent	filtrate	filtrate	water	water
CCDC	2054180	2032618	2054181	2032619

$_a R_1 = \sum ||F_o| - |F_c|| / \sum |F_o|, wR_2 = \left[\sum w(F_o^2 - F_c^2)^2 / \sum w(F_o^2)^2\right]^{1/2}$.

Table S2 Hydrogen bonds present in **1**

D–H···A	d(D–H)/Å	d(H–A)/Å	d(D–A)/Å	D–H–A/°
O1–H6···N6^{i}	0.82	1.80	2.583(2)	159.7
C3–H3···N3^{ii}	0.93	2.37	3.240(3)	156.2

Symmetry codes: (i) -1/2+x, 3/2-y, 1/2+z; (ii) 1/2+x, -1/2+y, +z.

Table S3 Hydrogen bonds present in **2**

D–H···A	d(D–H)/Å	d(H–A)/Å	d(D–A)/Å	D–H–A/°
N13–H13···O2^{i}	0.88	1.77	2.638(3)	167.3
N13–H13···N8^{i}	0.88	2.69	3.323(4)	129.7
N6–H6···O1^{ii}	0.88	1.76	2.602(3)	160.7
N6–H6···N1^{ii}	0.88	2.69	3.321(4)	129.8
N7–H7A···N1^{ii}	0.88(4)	2.29(4)	3.071(4)	149(3)
N14–H14A···N8^{i}	0.92(4)	2.17(4)	3.001(4)	149(3)
N7–H7B···O1^{iii}	0.98(4)	2.03(4)	2.963(4)	160(3)
N14–H14B···O2^{iv}	0.85(3)	2.63(3)	3.069(3)	114(3)
N14–H14B···N10^{iv}	0.85(3)	2.27(3)	3.088(4)	163(3)

Symmetry codes: (i) 1/2-x, -1/2+y, 1/2-z; (ii) 1/2-x, -1/2+y, -1/2-z; (iii) -x, 2-y, -1-z; (iv) 1-x, 2-y, 1-z.

Table S4 Hydrogen bonds present in **1b·H$_2$O**

D–H···A	d(D–H)/Å	d(H–A)/Å	d(D–A)/Å	D–H–A/°
N7–H7A···O2^{i}	0.83(5)	1.93(5)	2.761(3)	178(5)
N7–H7B···N1	0.85(5)	2.57(4)	3.170(3)	129(4)
N7–H7B···N3^{ii}	0.85(5)	2.57(5)	3.116(4)	124(4)
N7–H7C···N6^{iii}	0.89(5)	2.11(5)	3.000(3)	175(4)
N7–H7D···O1^{iv}	0.85(4)	1.97(4)	2.800(3)	168(5)
O2–H2A···O1^{v}	0.82(2)	1.91(2)	2.710(3)	166(5)
O2–H2B···N5^{vi}	0.83(2)	2.02(2)	2.843(3)	170(5)

symmetry codes: (i) 1/2+x, 1/2-y, -1/2+z; (ii) -1/2+x, 1/2+y, +z; (iii) -1+x, 1-y, -1/2+z; (iv) 1/2+x, 1/2+y, +z; (v) 1/2+x, 1/2-y, 1/2+z; (vi) -1+x, +y, +z.

Table S5 Hydrogen bonds present in **2e·H$_2$O**

D–H···A	d(D–H)/Å	d(H–A)/Å	d(D–A)/Å	D–H–A/°
O2–H2A···O1^{i}	0.83(3)	2.06(3)	2.892(4)	172(5)
O2–H2B···N3^{ii}	0.84(3)	2.10(3)	2.930(4)	170(6)
N10–H10A···O2^{iii}	0.86	2.64	3.044(5)	110.4
N10–H10A···N2^{iii}	0.86	2.42	3.189(5)	149.1
N10–H10B···O1	0.86	2.27	3.131(5)	174.1

N8–H8A···N6^{iv}	0.86	2.18	3.020(4)	165.3
N8–H8B···N5	0.86	2.08	2.920(4)	165.2
N9–H9A···N3^{iii}	0.86	2.43	3.285(5)	174.1
N9–H9A···N2^{iii}	0.86	2.38	3.161(5)	151.4
N9–H9B···O1^{iv}	0.86	2.12	2.963(5)	167.4
N1–H1A···N4^{ii}	0.86	2.59	3.151(5)	123.5
N1–H1B···O2	0.86	2.03	2.891(5)	177.6

symmetry codes: (i) -1+x, -1+y, -1+z; (ii) +x, -1+y, +z; (iii) 2+x, 1+y, 1+z; (iv) +x, 1+y, +z.

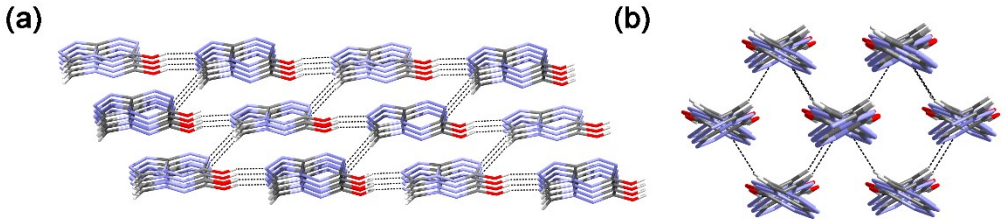

Fig. S1 (a) The strong intermolecular hydrogen bonds in **1**. (b) Packing diagram of **1** viewed along *a* axis.

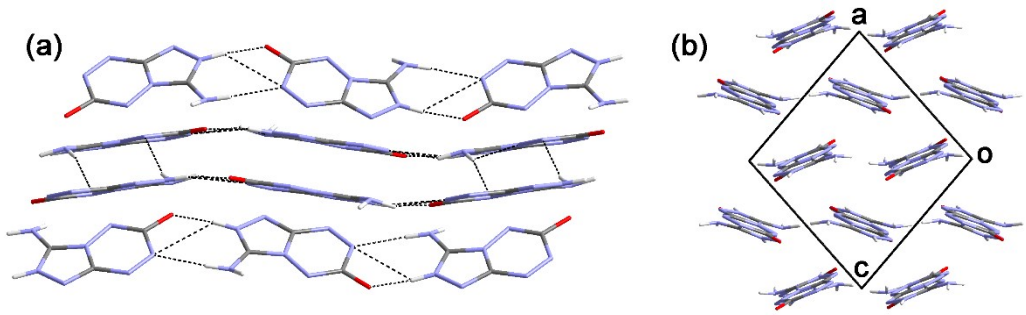

Fig. S2 (a) The strong intermolecular hydrogen bonds in **2**. (b) The packing diagram of **2** viewed along *b* axis.

2. Computational details

Noncovalent interactions and molecular electrostatic potential analyses were carried out by Multiwfn (3.3.9) and visualized by VMD (1.9.3).[1] Hirshfeld surfaces analyses and the 2D fingerprint plots were obtained from using CrystalExplorer (17.5).[2] Surfaces mapped with d_{norm} for **1, 1b·H$_2$O, 2, 2e·H$_2$O** are depicted in Fig. S3. Theoretical calculations were carried out by using Gaussian 16 program (Revision C.01). The geometric optimization and frequency analyses of all the compounds were performed at the level of B3LYP functional

with 6-31+G** basis set. Single-point energies were calculated at MP2/6-311++G** level.[3] All of the optimized structures were determined to be true local energy minima on the potential-energy surface without imaginary frequencies. The heat of formation (HOF) of compound **1**, 3,5-diaminotriazole cation, zwitterionic salt **2** and its anion was obtained using isodesmic reactions, which was shown in Scheme S1. Besides, the HOF for other compounds were obtained by using G2 ab initio method based on atomization reaction and NIST WebBook.[4,5] The calculation results of the gas-phase species were list in Table S6.

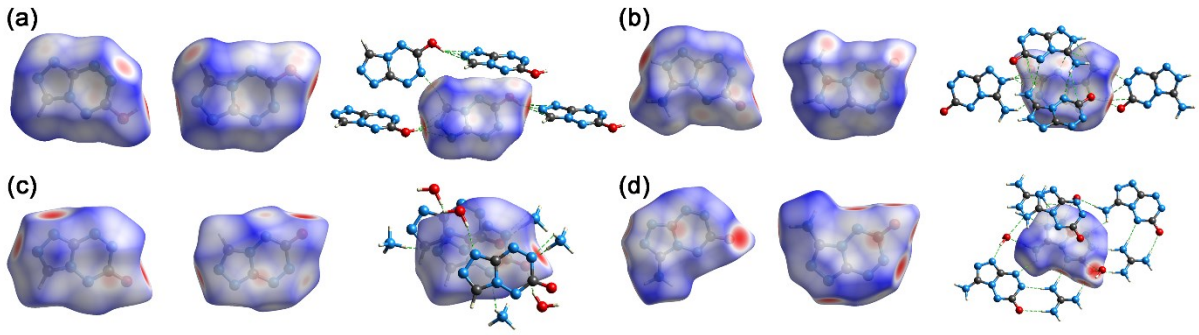

Fig. S3 Hirshfeld surfaces of **1** (a)**, 2** (b)**, 1b·H$_2$O** (c) and **2e·H$_2$O** (d) mapped with d_{norm}. Close contacts are depicted as green dash lines.

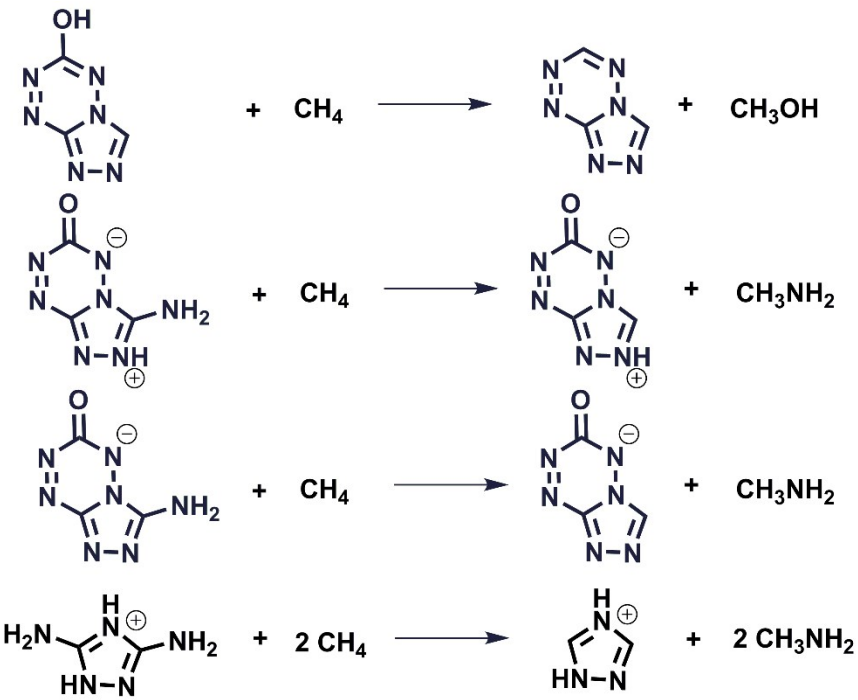

Scheme S1. Isodesmic reactions for calculating the HOF of compound **1**, 3,5-diaminotriazole cation, zwitterionic salt **2** and its anion.

Table S6 Calculated HOF of the gas-phase species

Compound	ΔH_f° (kJ·mol^{-1})	Compound	ΔH_f° (kJ·mol^{-1})
CH_3NH_2	-23.50	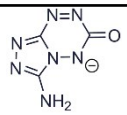	249.04
CH_4	-74.87	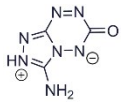	532.90
	192.70[a]	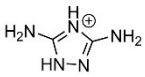	793.24
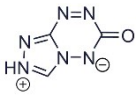	546.44		

[a] Ref. 5.

For neutral compound **1** and **2**, the solid-phase HOF were obtained by subtracting the heat of sublimation (ΔH_{sub}) from its gas-phase HOF. Based on Trouton's rule, the solid-phase HOF of **1** and **2** were calculated by equation 1, where T denotes either the melting point or the decomposition temperature when no melting occurs before the decomposition.[6]

$$\Delta H_f(s) = \Delta H_f(g) - \Delta H_{sub} = \Delta H_f(g) - 188[J \cdot mol \cdot K^{-1}] \times T \quad (1)$$

For other energetic salts, the solid-phase HOF were calculated on the basis of Born-Haber energy cycle, which is shown in Scheme S2. The calculation equation is simplified by using equation 2.

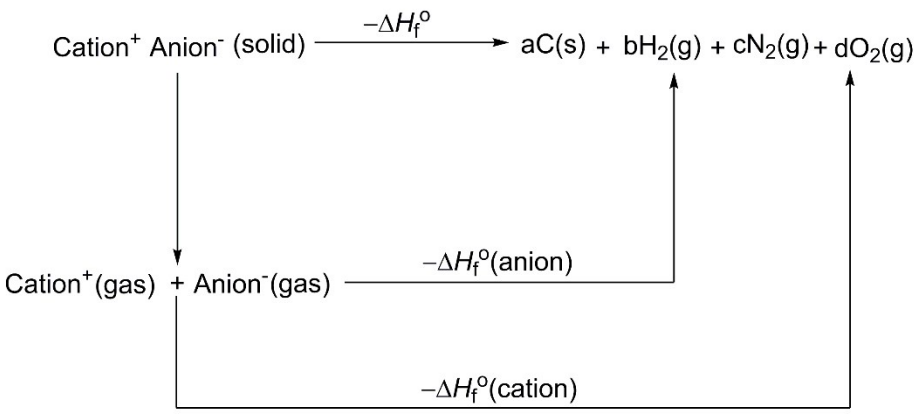

Scheme S2 Born-Haber energy cycle for the formation of energetic salts.

$$\Delta H_f^o(salt, 298\ K) = \Delta H_f^o(cation, 298\ K) + \Delta H_f^o(anion, 298\ K) - \Delta H_L \quad (2)$$

In equation 2, ΔH_L represents the lattice energy of the ionic salts and it can be obtained by using equation 3 that suggested by Jenkins, et al.[7]

$$\Delta H_L = U_{pot} + [p\left(\frac{n_M}{2} - 2\right) + q(\frac{n_X}{2} - 2)]RT \quad (3)$$

In equation 3, the values of n_M and n_X depend on the nature of the ions (M^{q+} and X^{P-}), which equal to 3 for monatomic ions, 5 for linear polyatomic ions, and 6 for nonlinear polyatomic ions. In this equation, U_{pot} represents the lattice potential energy that can be calculated from equation 4:

$$U_{pot}(kJ \cdot mol^{-1}) = \gamma(\rho_m/M_m)^{1/3} + \delta \quad (4)$$

where ρ_m equals to the density of the energetic salt and M_m denotes the chemical formula mass of the compound. Besides, the values of coefficients γ $(kJ \cdot mol^{-1} \cdot cm)$ and δ $(kJ \cdot mol^{-1})$ can be assigned according to the literature.[7]

Based on the measured densities and the calculated heats of formation, the detonation velocities and detonation pressures of all the compounds were evaluated using EXPLO5 v6.04, and the results are summarized in Table 1.

3. NMR spectra

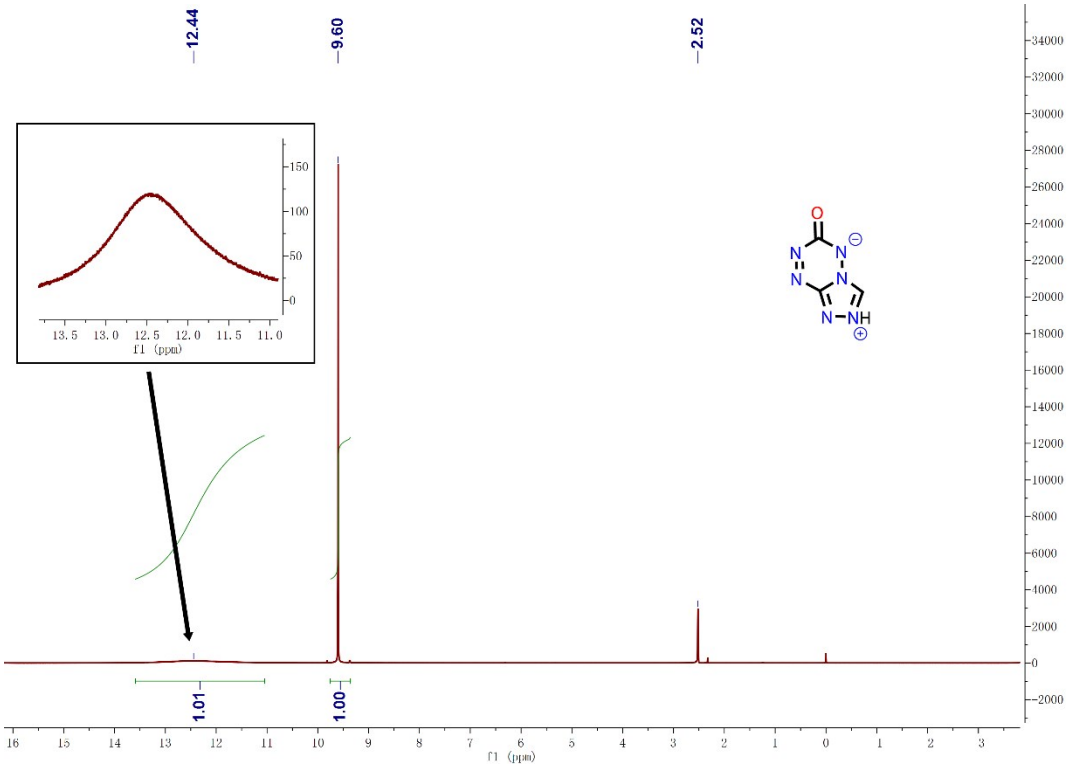

Fig. S4 ^{1}H NMR spectrum of **1**.

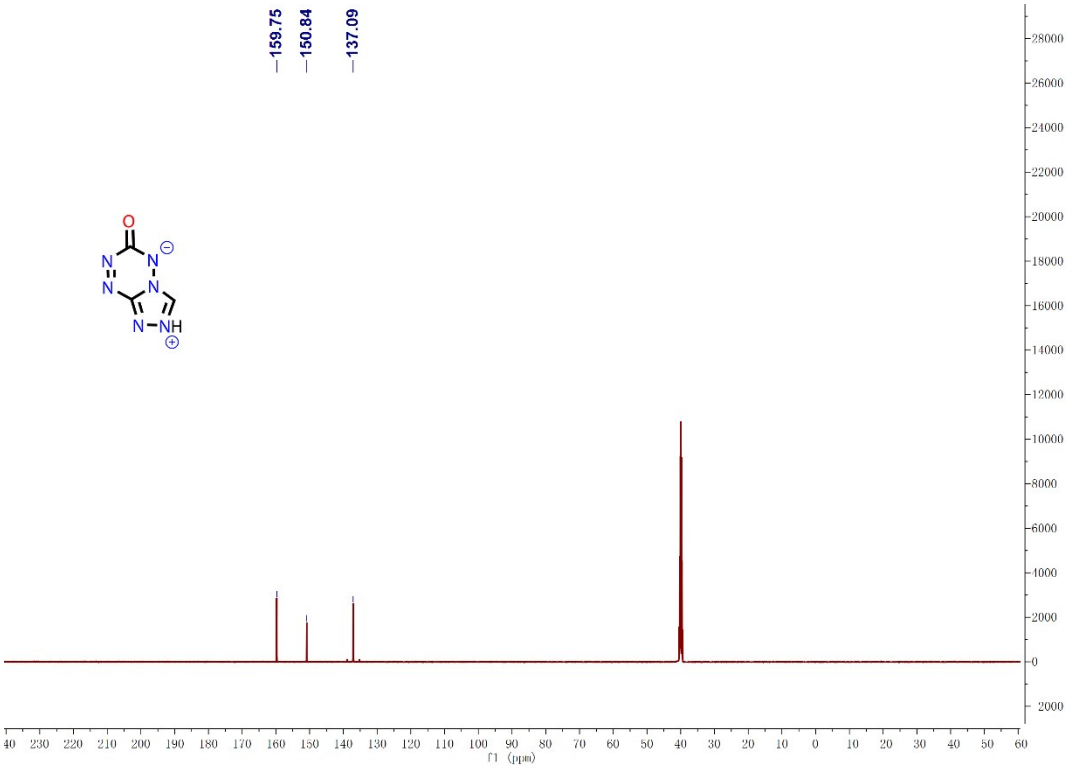

Fig. S5 ^{13}C NMR spectrum of **1**.

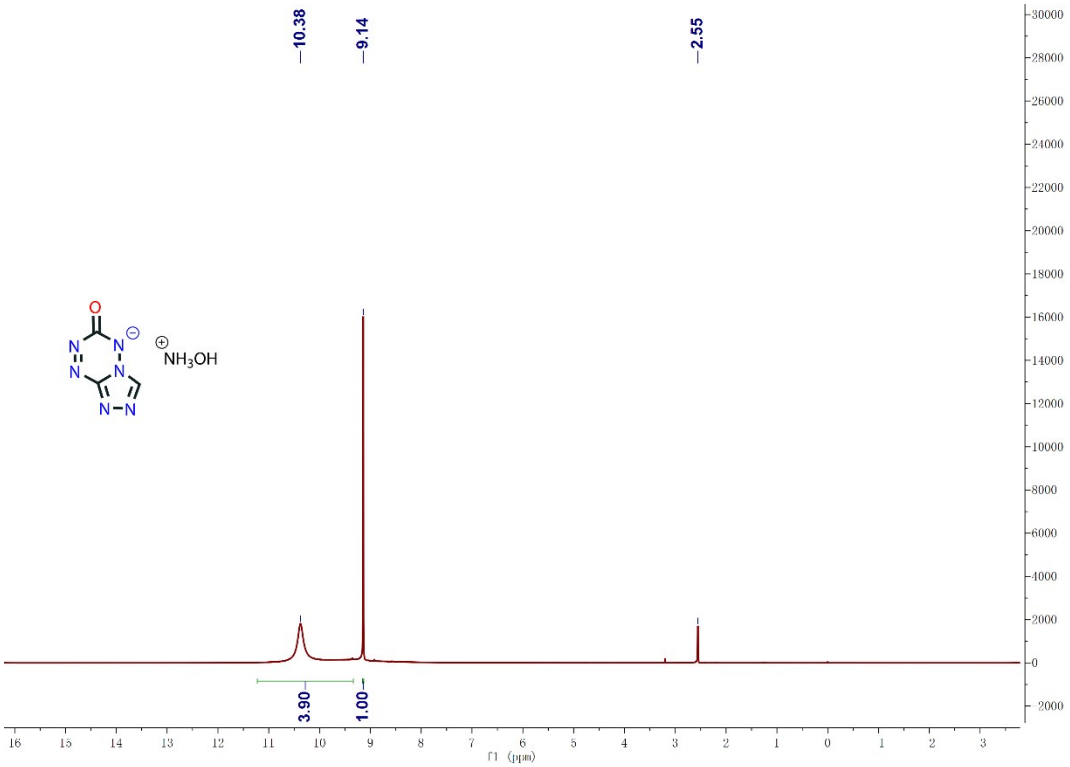

Fig. S6 ^{1}H NMR spectrum of **1a**.

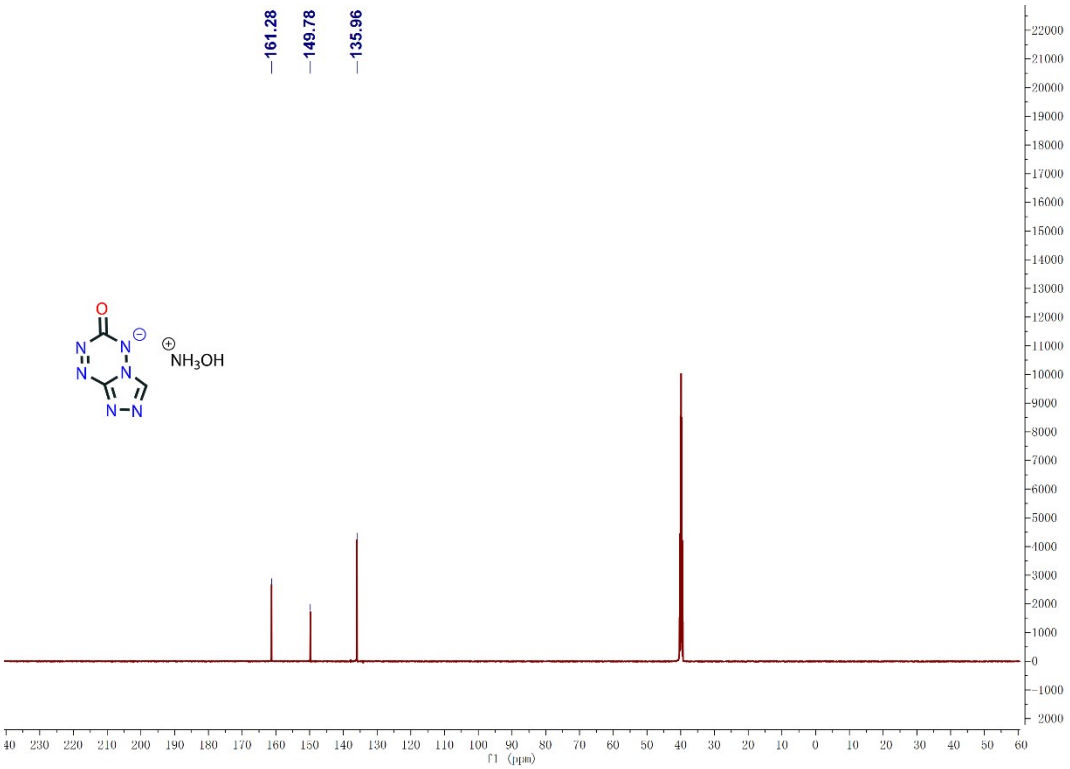

Fig. S7 ^{13}C NMR spectrum of **1a**.

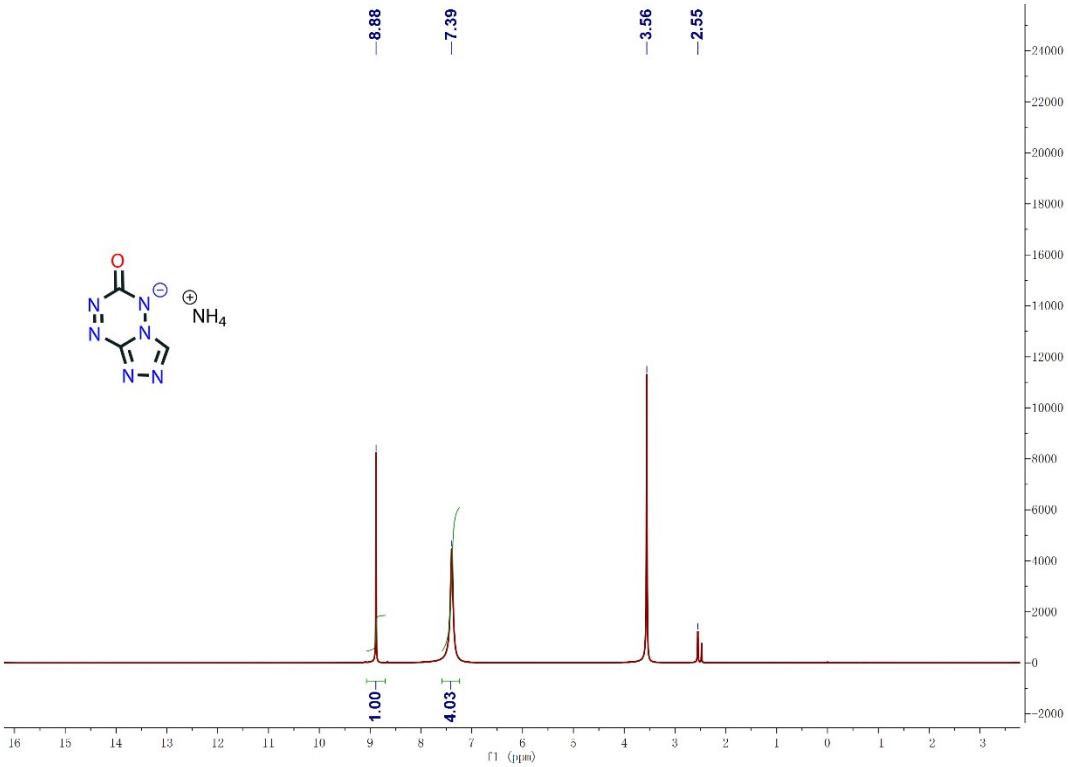

Fig. S8 ^{1}H NMR spectrum of **1b**.

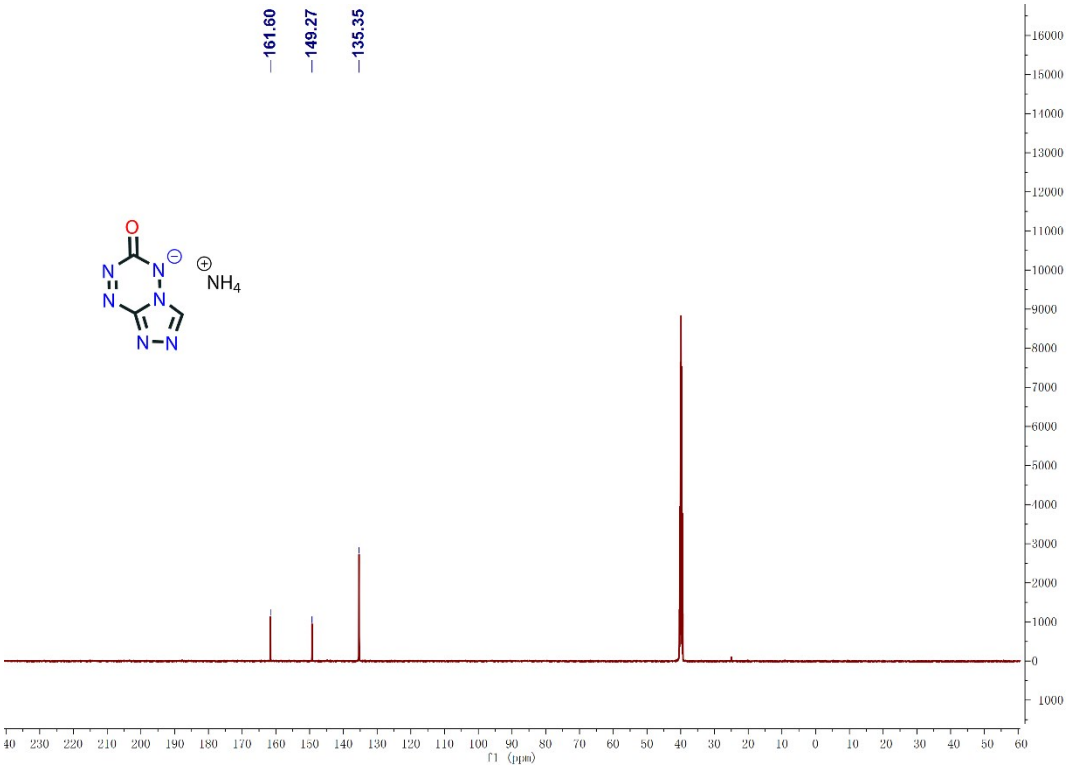

Fig. S9 ^{13}C NMR spectrum of **1b**.

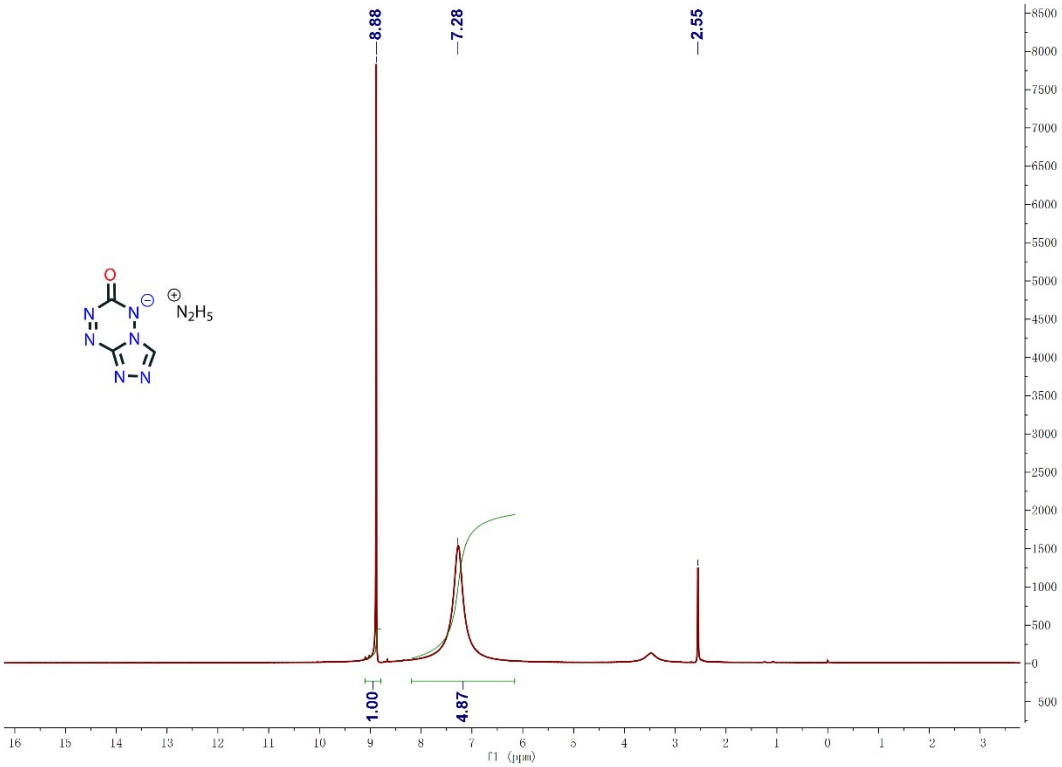

Fig. S10 ^{1}H NMR spectrum of **1c**.

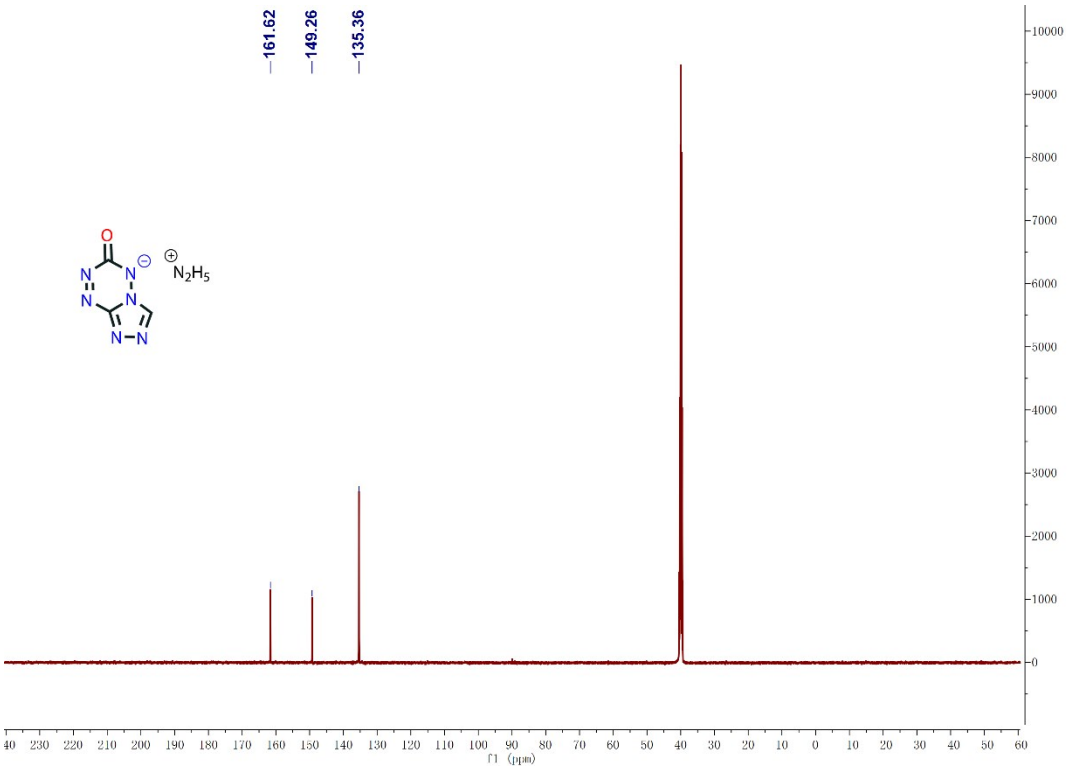

Fig. S11 ^{13}C NMR spectrum of **1c**.

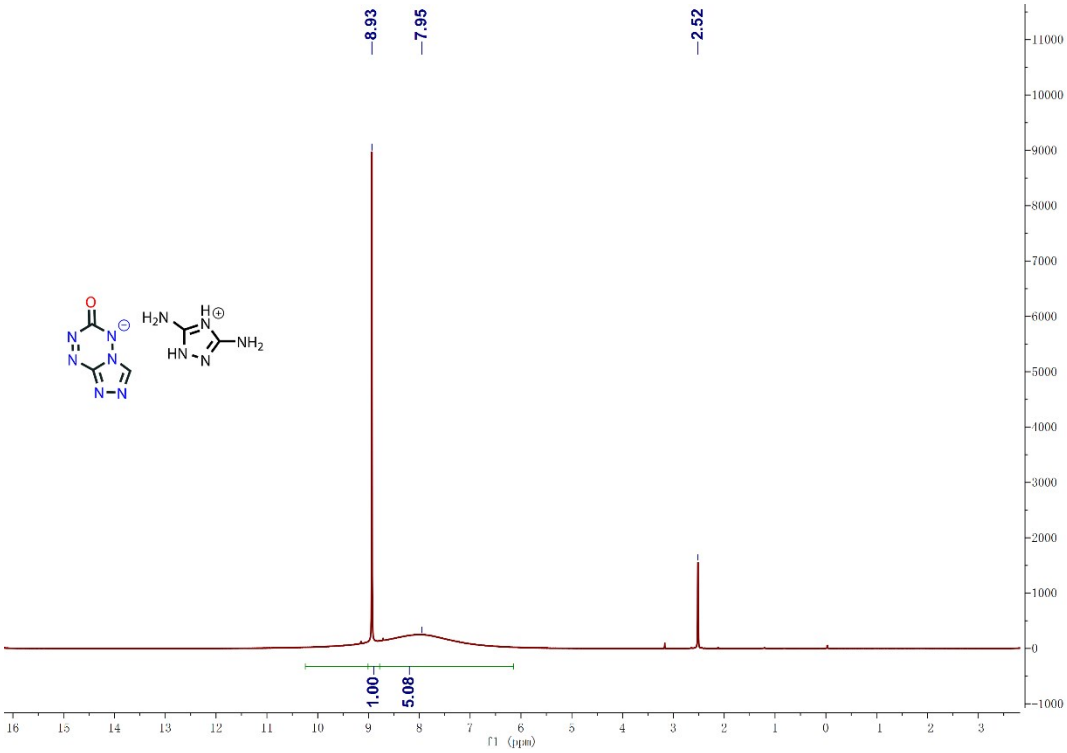

Fig. S12 ^{1}H NMR spectrum of **1d**.

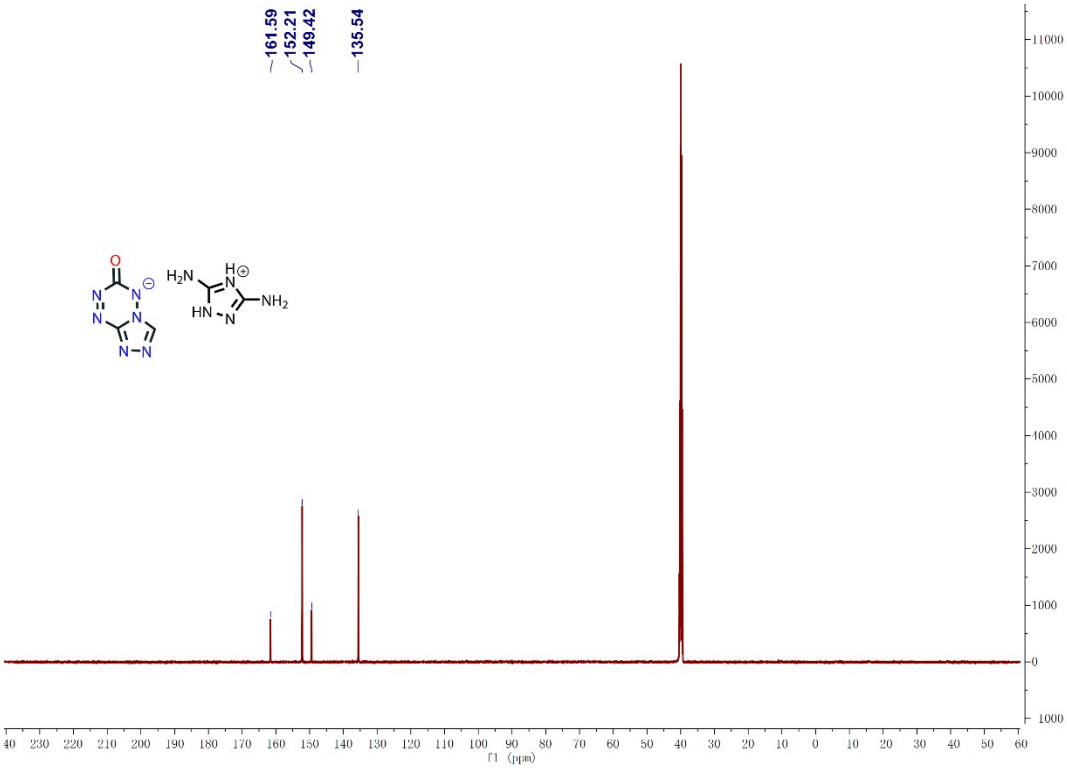

Fig. S13 ^{13}C NMR spectrum of **1d**.

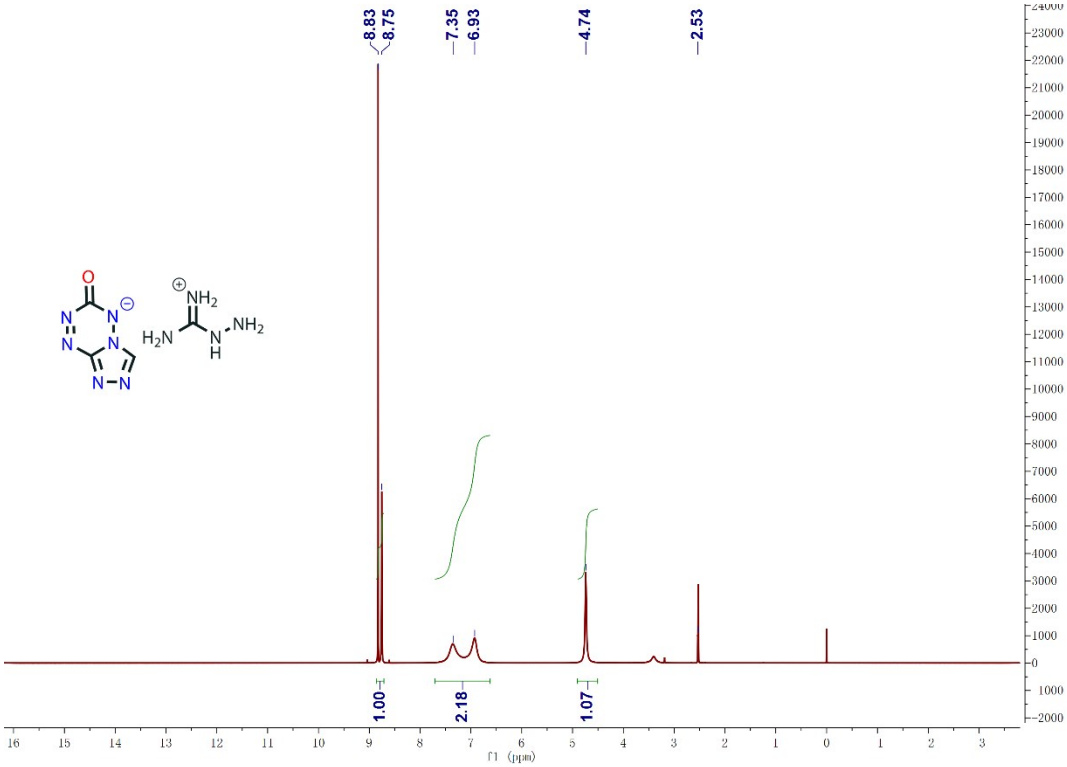

Fig. S14 ^{1}H NMR spectrum of **1e**.

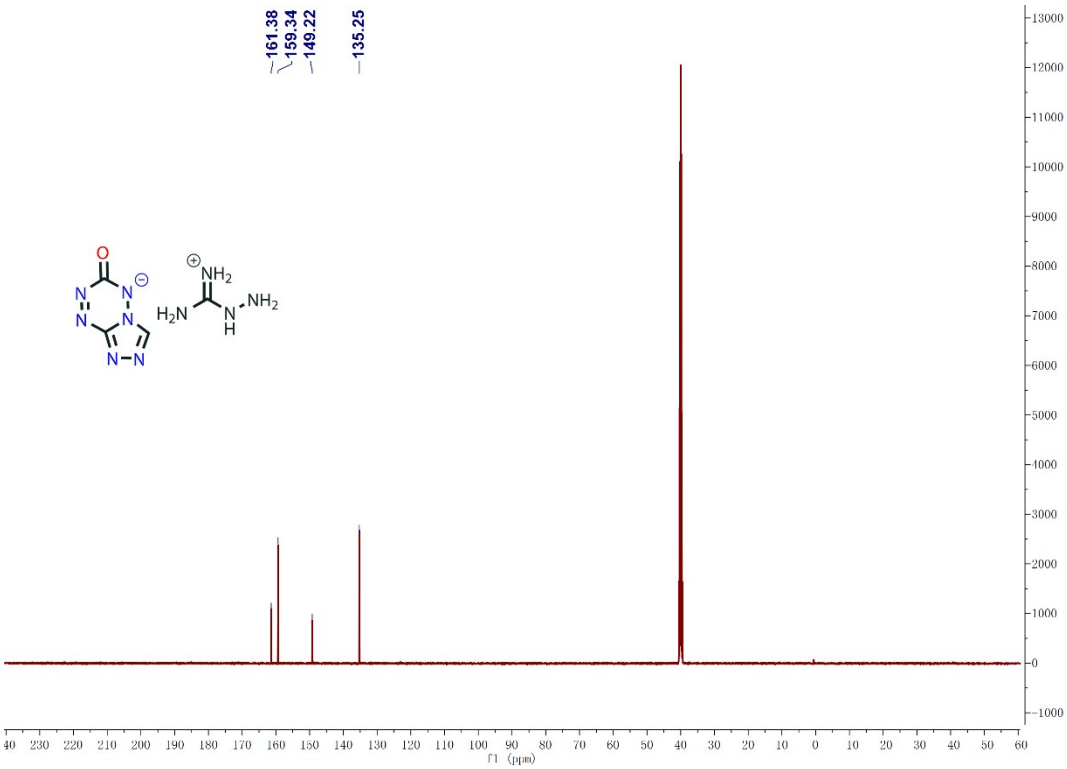

Fig. S15 ^{13}C NMR spectrum of **1e**.

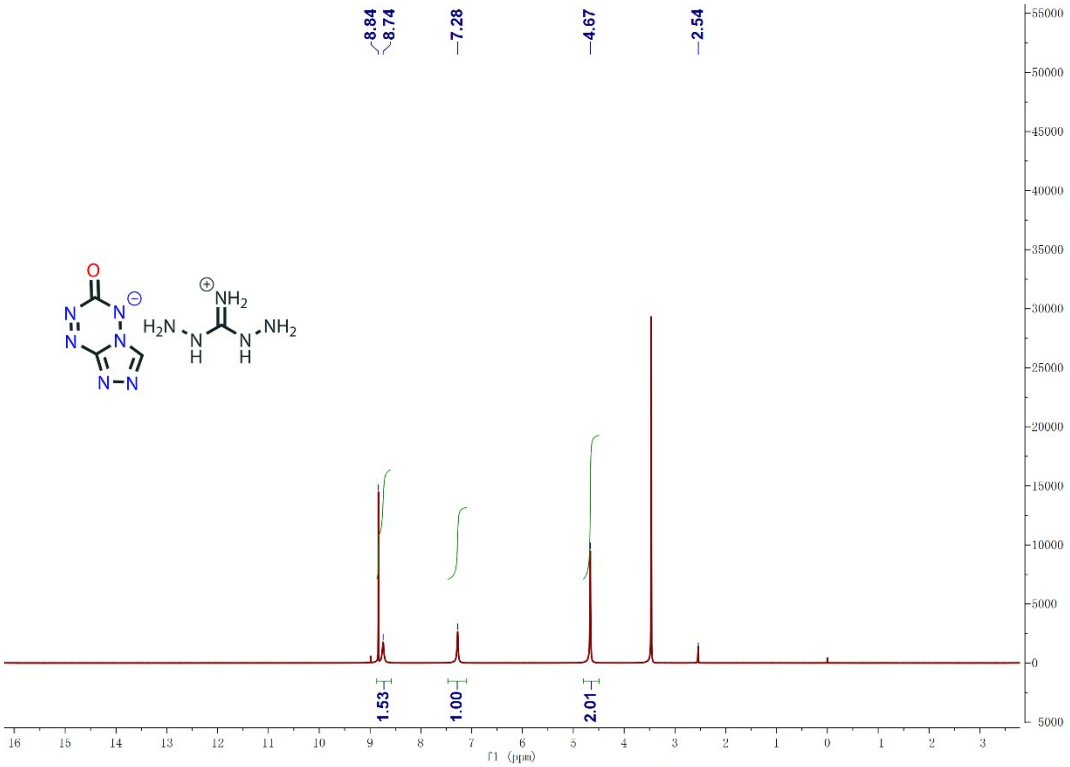

Fig. S16 ^{1}H NMR spectrum of **1f**.

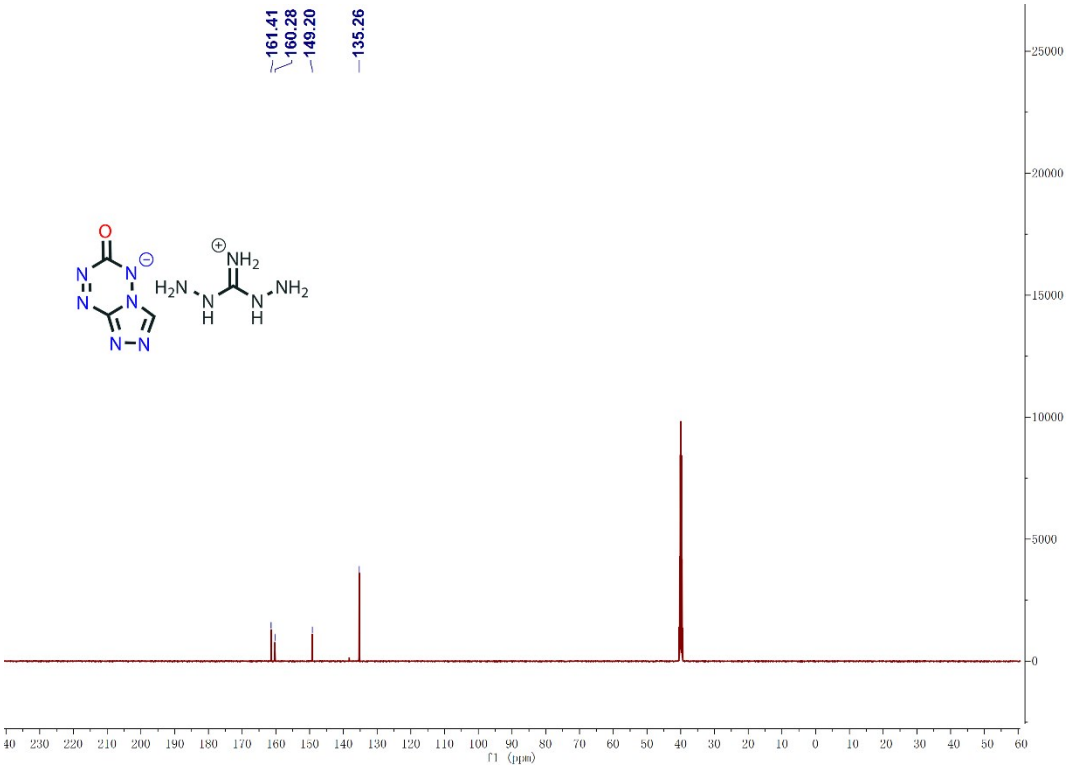

Fig. S17 ^{13}C NMR spectrum of **1f**.

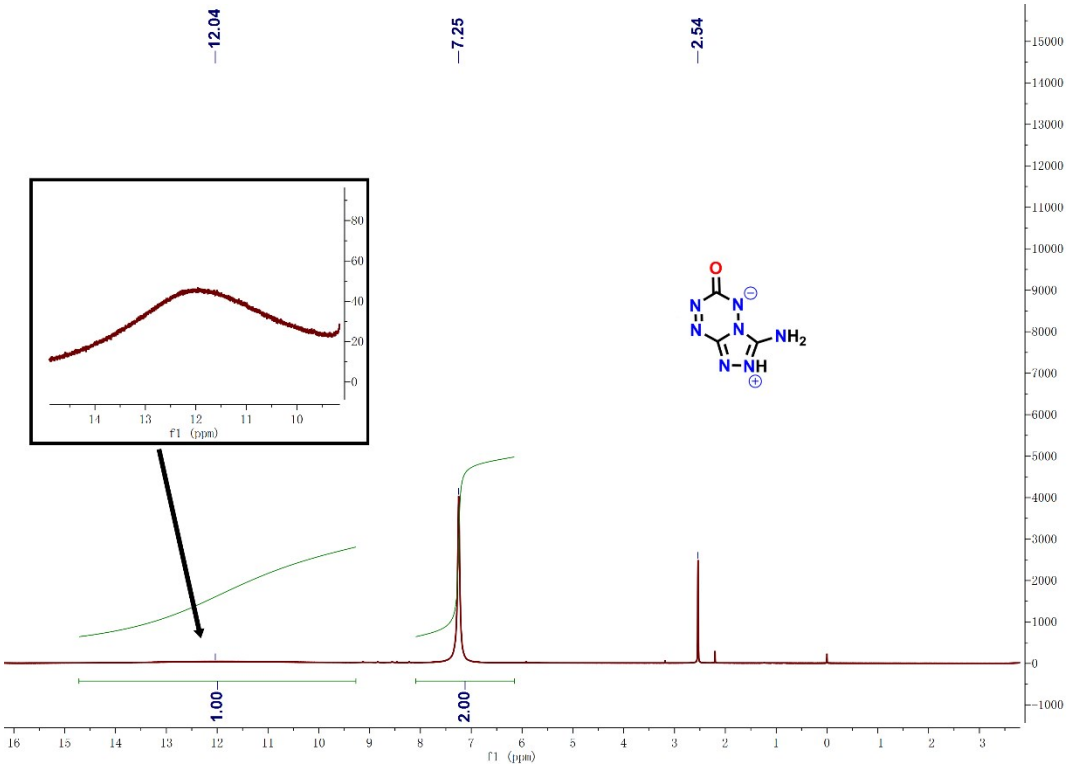

Fig. S18 ^{1}H NMR spectrum of **2**.

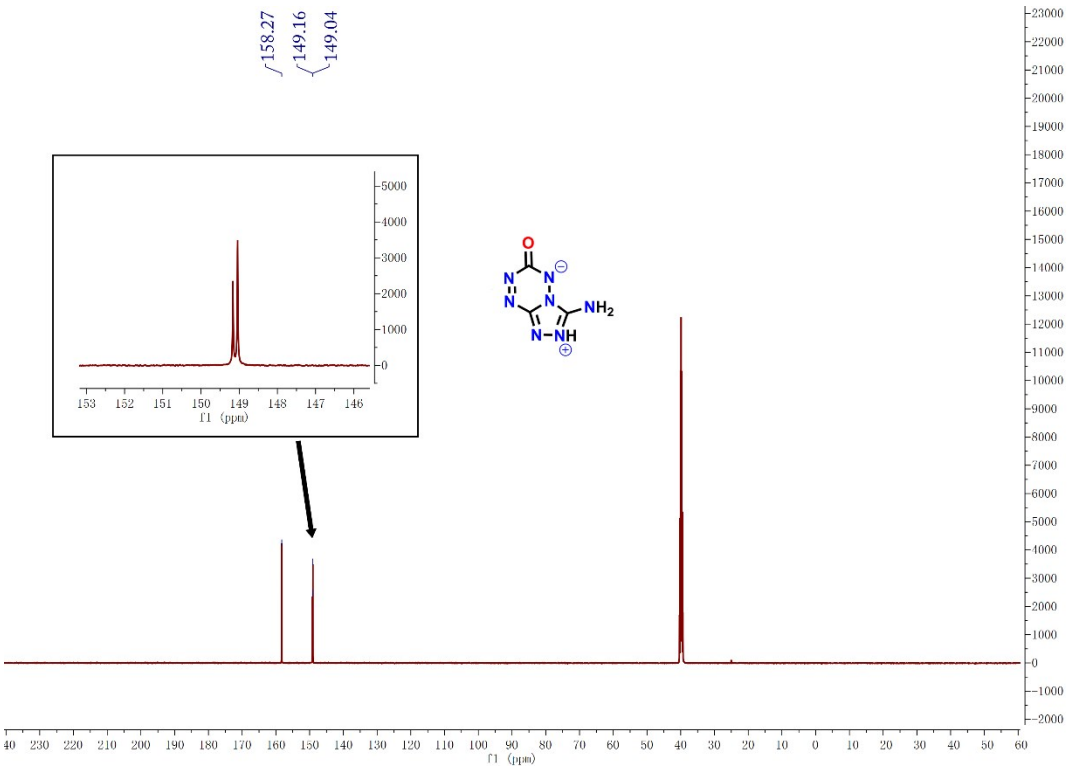

Fig. S19 ^{13}C NMR spectrum of **2**.

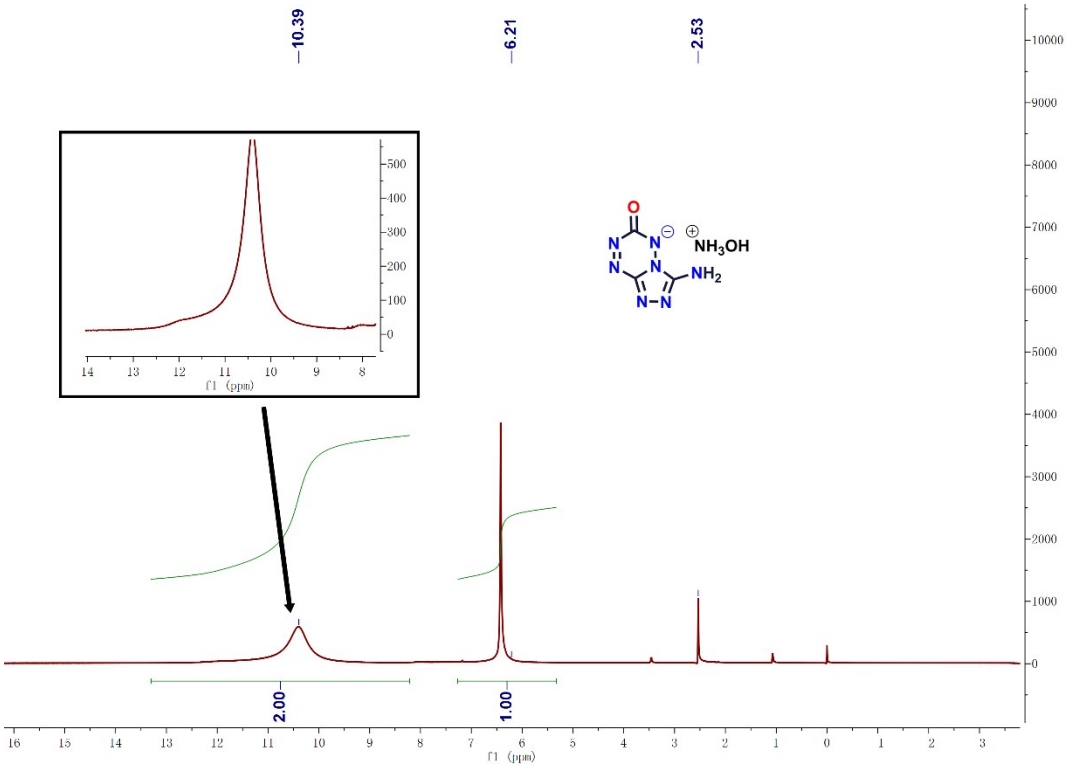

Fig. S20 ^{1}H NMR spectrum of **2a**

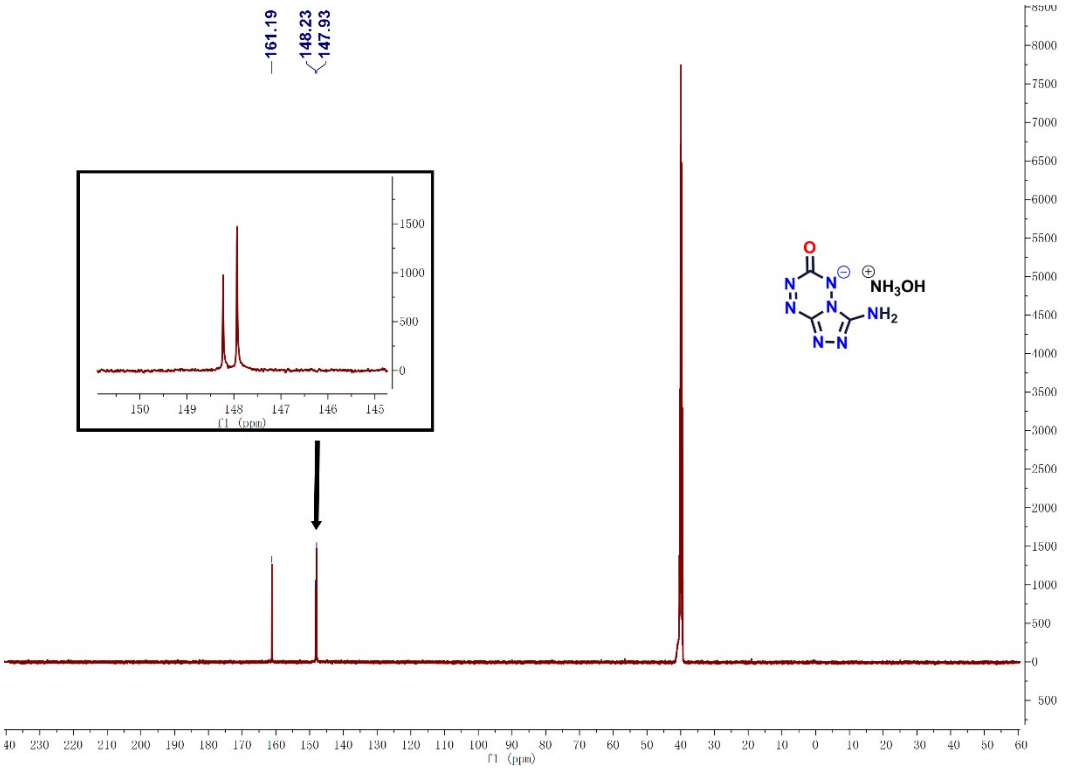

Fig. S21 ^{13}C NMR spectrum of **2a**.

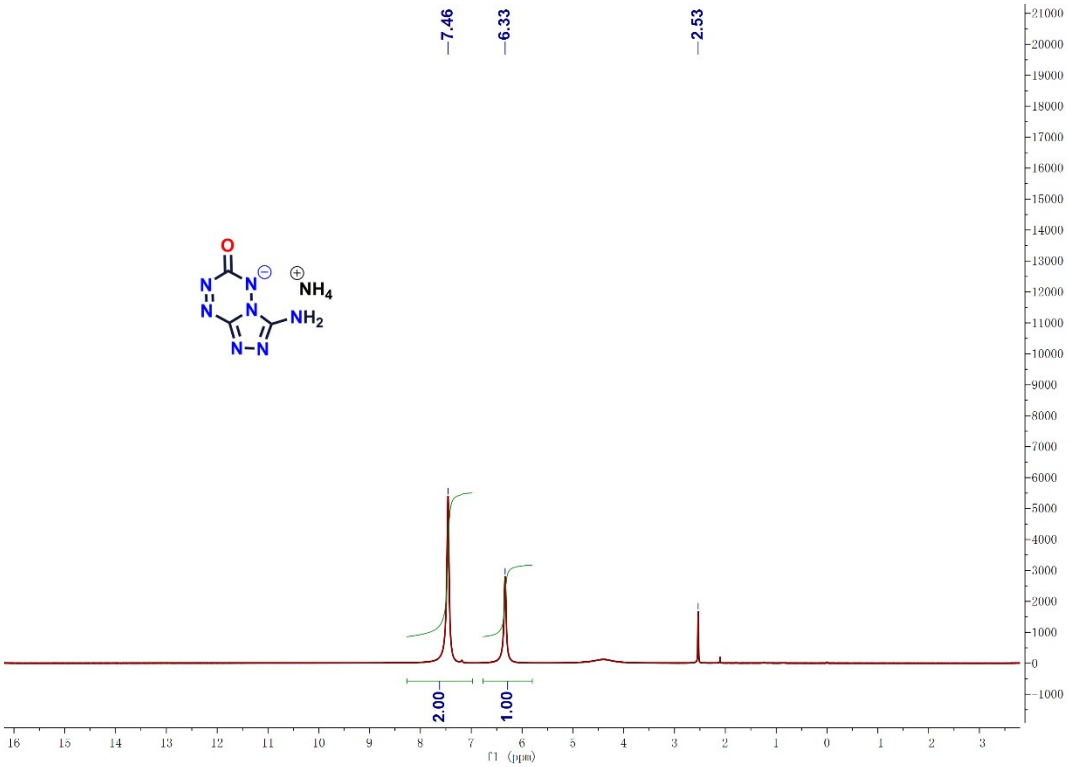

Fig. S22 ^{1}H NMR spectrum of **2b**.

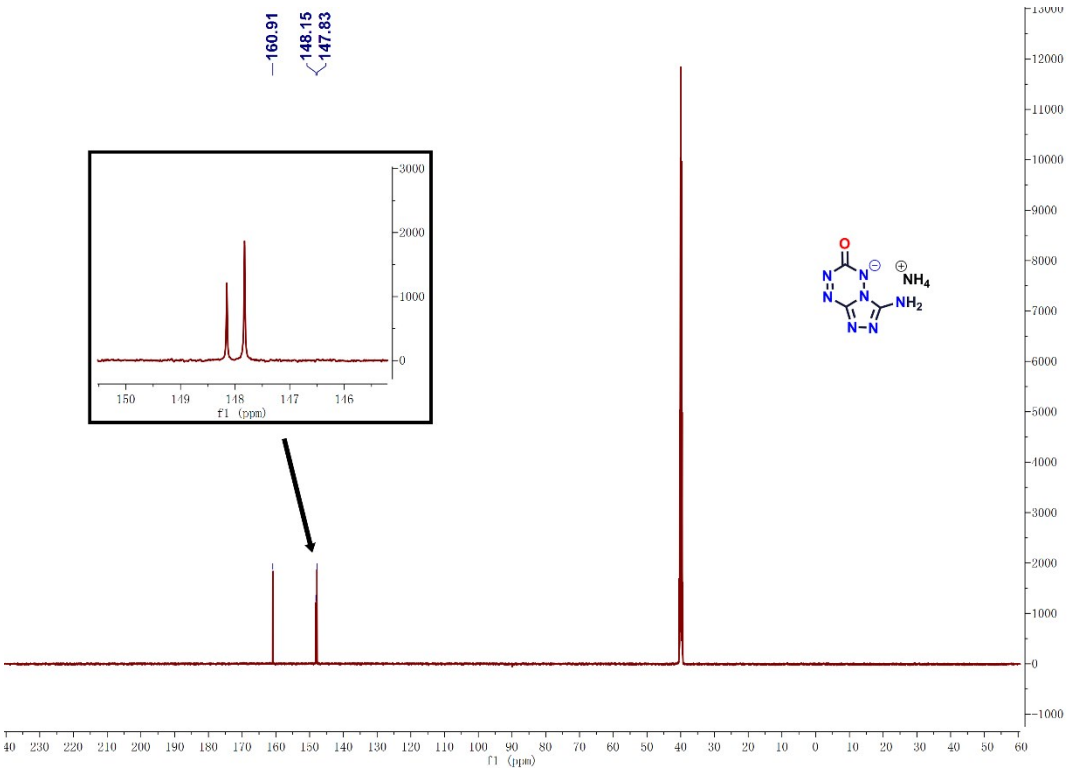

Fig. S23 ^{13}C NMR spectrum of **2b**.

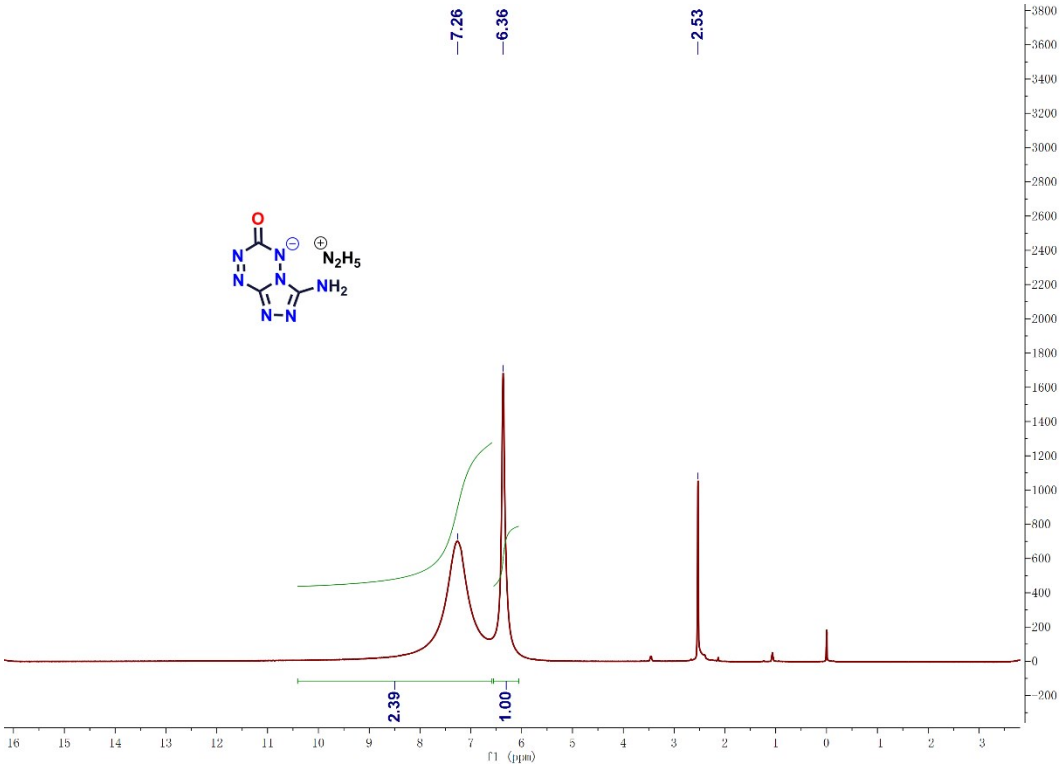

Fig. S24 ^{1}H NMR spectrum of **2c**.

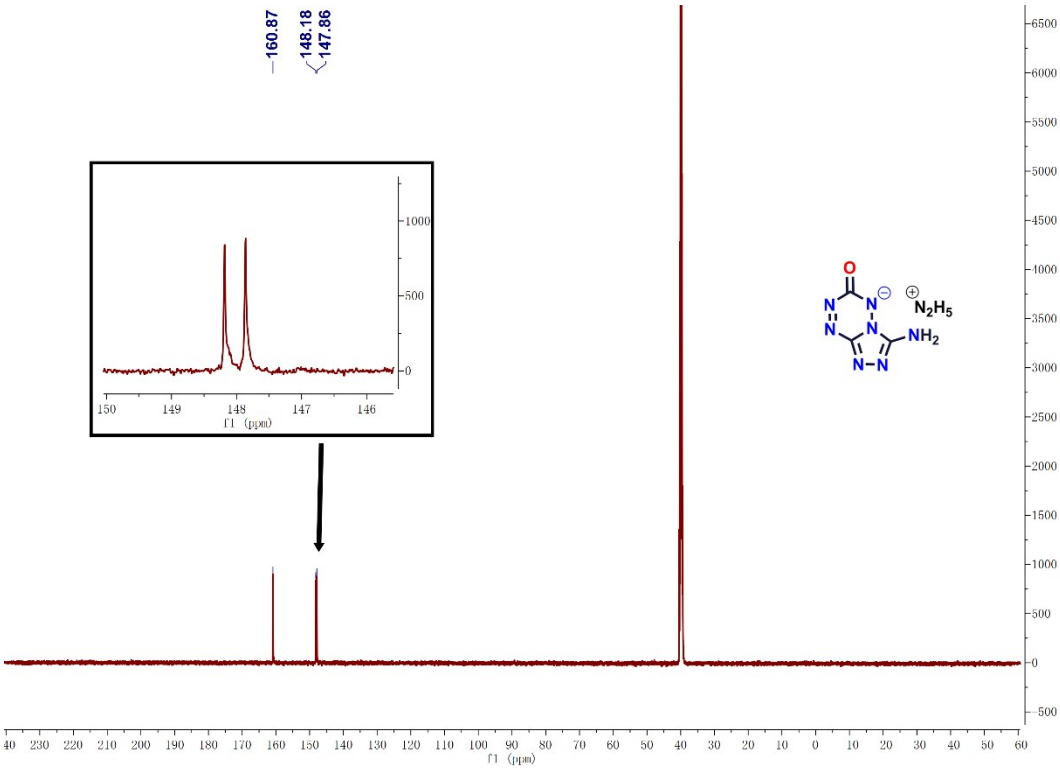

Fig. S25 ^{13}C NMR spectrum of **2c**.

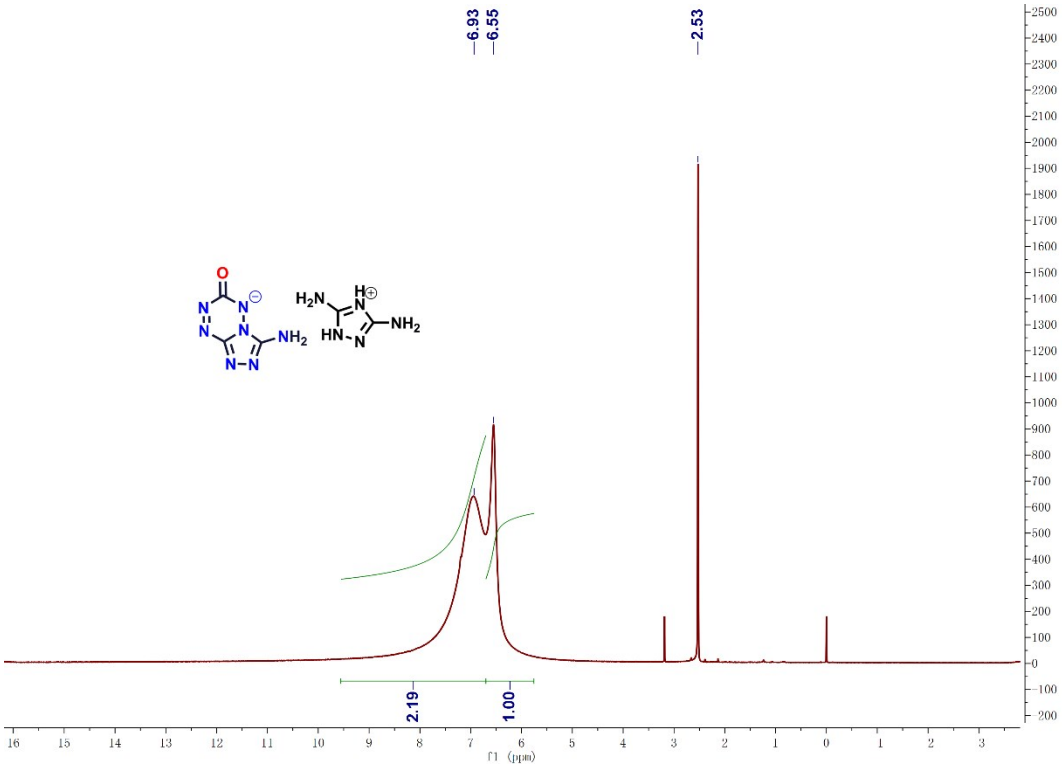

Fig. S26 ^{1}H NMR spectrum of **2d**.

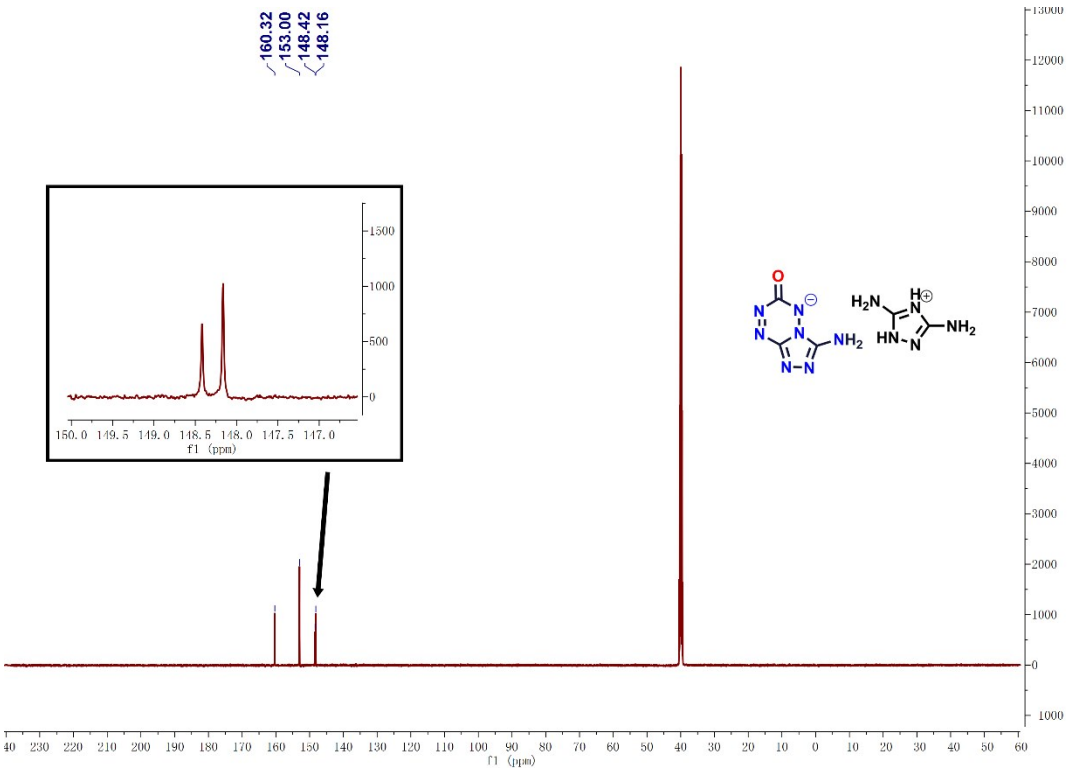

Fig. S27 ^{13}C NMR spectrum of **2d**.

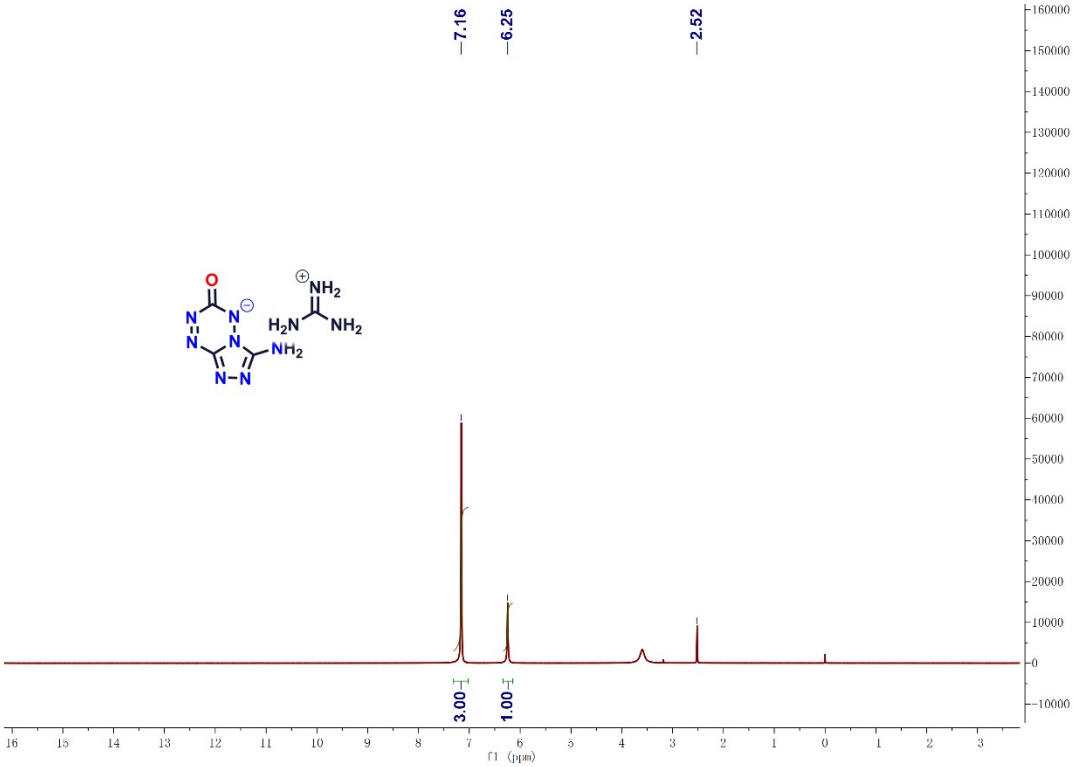

Fig. S28 ^{1}H NMR spectrum of **2e.**

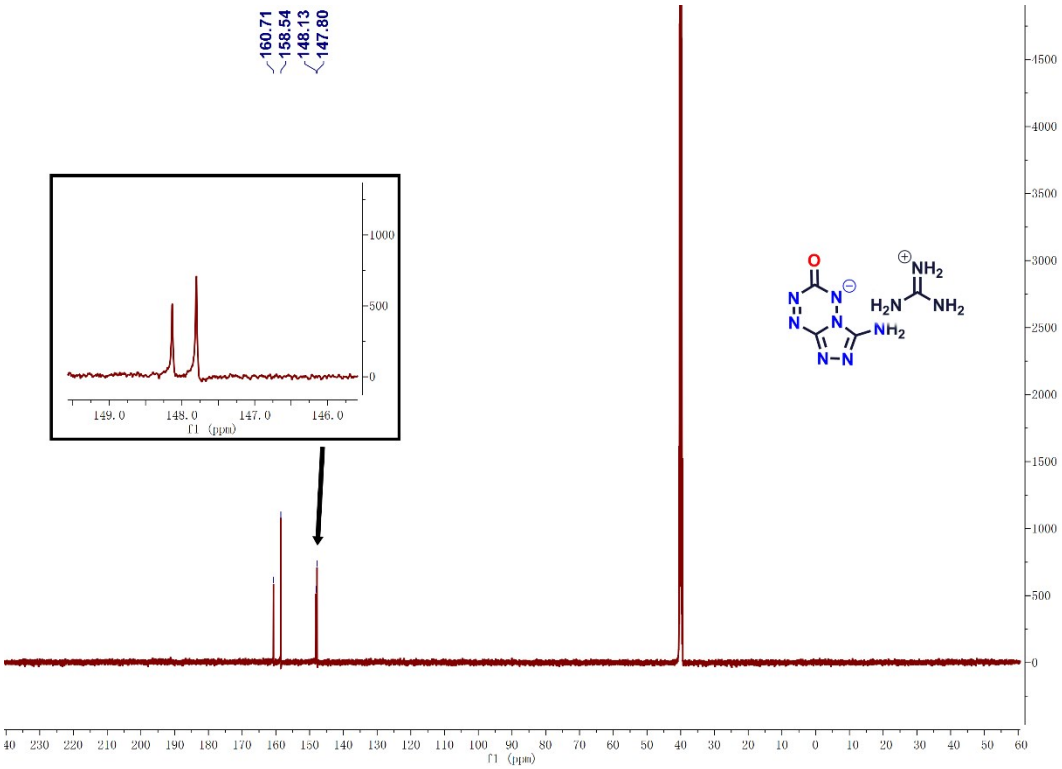

Fig. S29 ^{13}C NMR spectrum of **2e**.

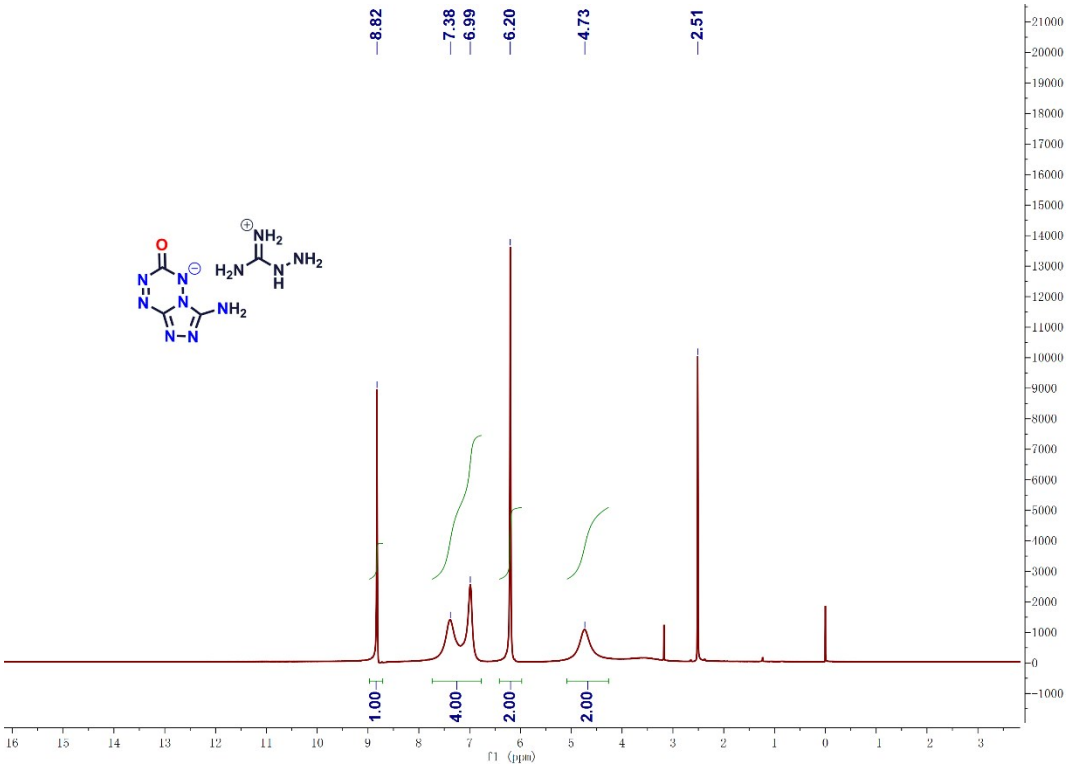

Fig. S30 ^{1}H NMR spectrum of **2f**.

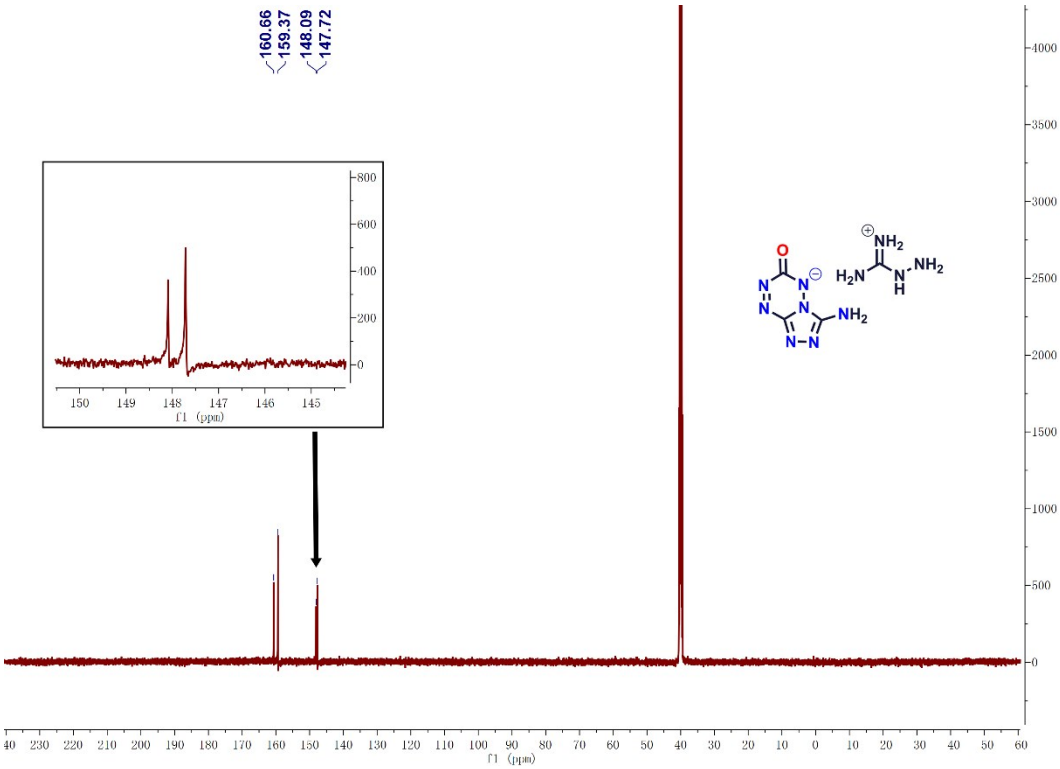

Fig. S31 ^{13}C NMR spectrum of **2f**.

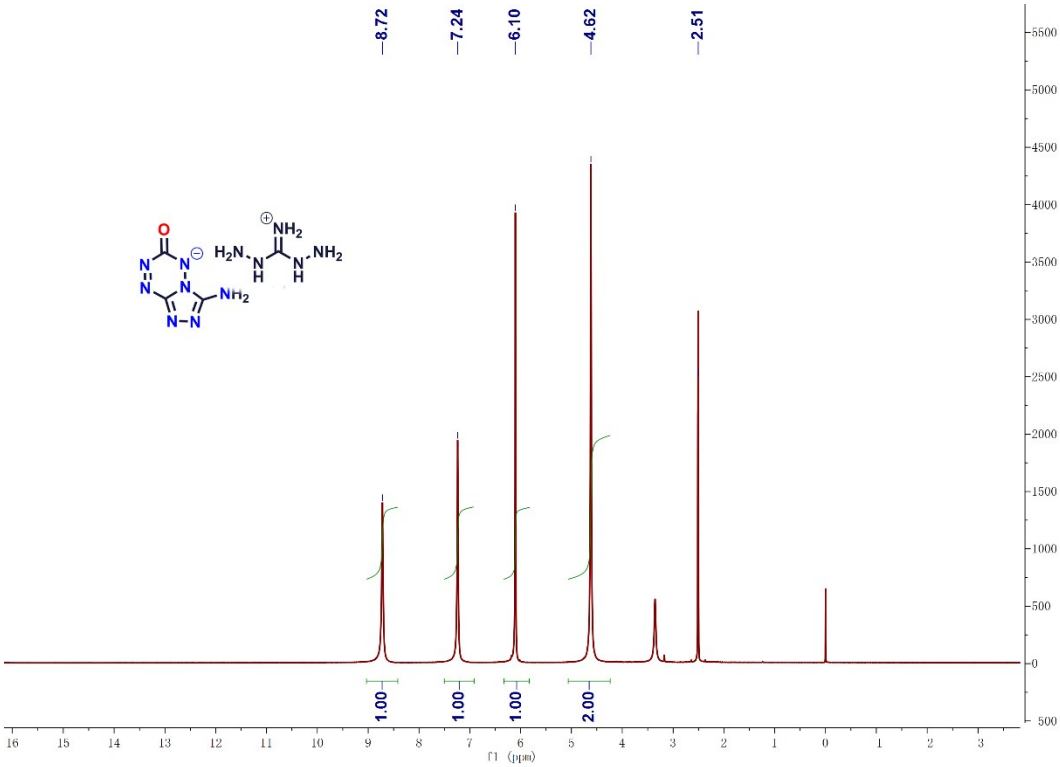

Fig. S32 ^{1}H NMR spectrum of **2g**.

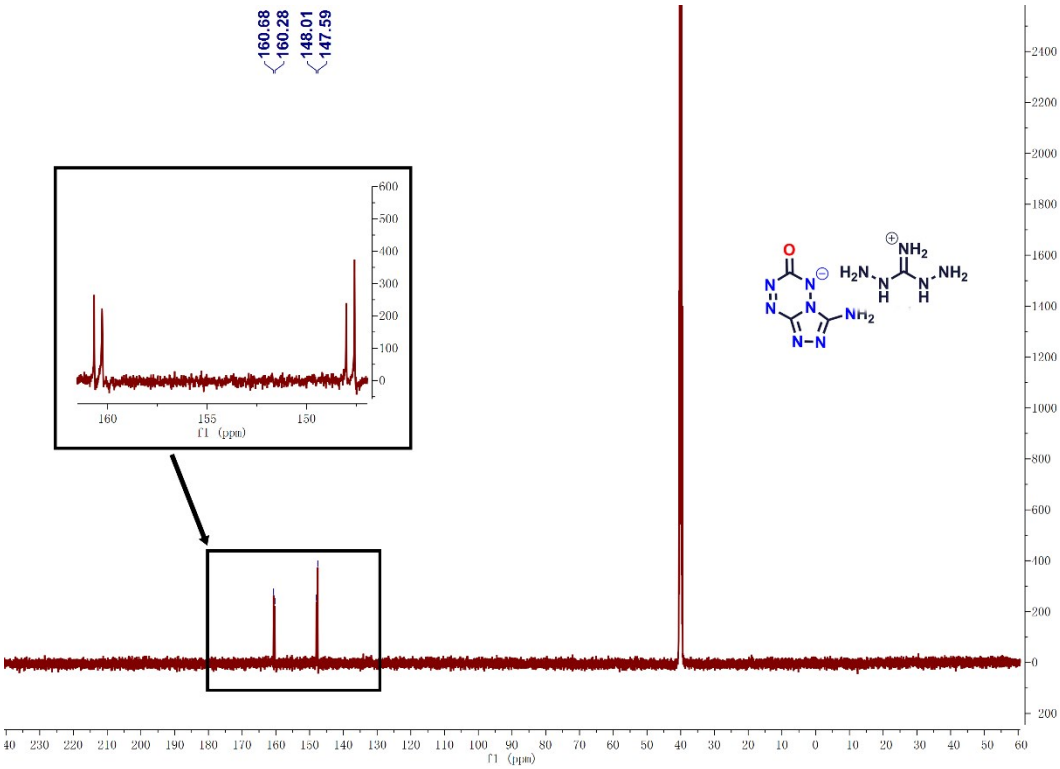

Fig. S33 ^{13}C NMR spectrum of **2g**.

4. References.

1 W. Humphrey, A. Dalke and K. Schulten, *J. Mol. Graphics Modell.*, 1996, **14**, 33.

2 M. J. Turner, J. J. McKinnon, S. K. Wolff, D. J. Grimwood, P. R. Spackman, D. Jayatilaka and M. A. Spackman, *CrystalExplorer17*, University of Western Australia, 2017.

3 R. G. Parr and W. Yang, *Density Functional Theory of Atoms and Molecules*, Oxford University Press: Oxford, U.K., 1989.

4 L. A. Curtiss, K. Raghavachari, G. W. Trucks and J. A. Pople, *J. Chem. Phys.*, 1991, **94**, 7221- 7230.

5 NIST Chemistry WebBook, https://webbook.nist.gov/chemistry/, (accessed April 2021).

6 M. S. Westwell, M. S. Searle, D. J. Wales and D. H. Wiliams, *J. Am. Chem. Soc.*, 1995, **117**, 5013.

7 H. D. B. Jenkins, D. Tudela and L. Glasser, *Inorg. Chem.*, 2002, **41**, 2364-2367.